Cell Reports, Volume *36*

Supplemental information

Substrate ubiquitination retains misfolded membrane proteins in the endoplasmic reticulum for degradation

Zhihao Sun, Christopher J. Guerriero, and Jeffrey L. Brodsky

Figure S1

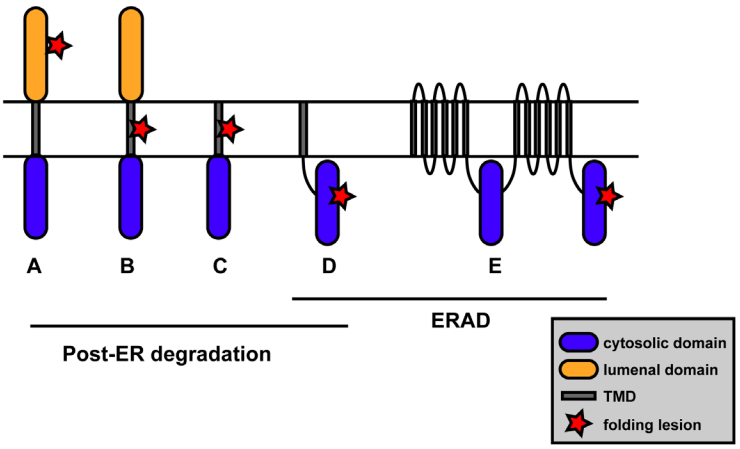

	A	B	C	D	E
Proteins	Wsc1*, CFS	Pep12(D)	CPS1, Phm5	SZ*	Ste6*
Normal residence	PM/ ND	LE	vacuole	ND	PM
Site of proteolysis	vacuole			vacuole/ proteasome	proteasome
E3 ligase	Rsp5	Tul1		Doa10	

Figure S1. Degradative fates of select membrane proteins in yeast. Related to Figure 1. See main text for additional details; ND, not determined or not applicable.

Figure S2

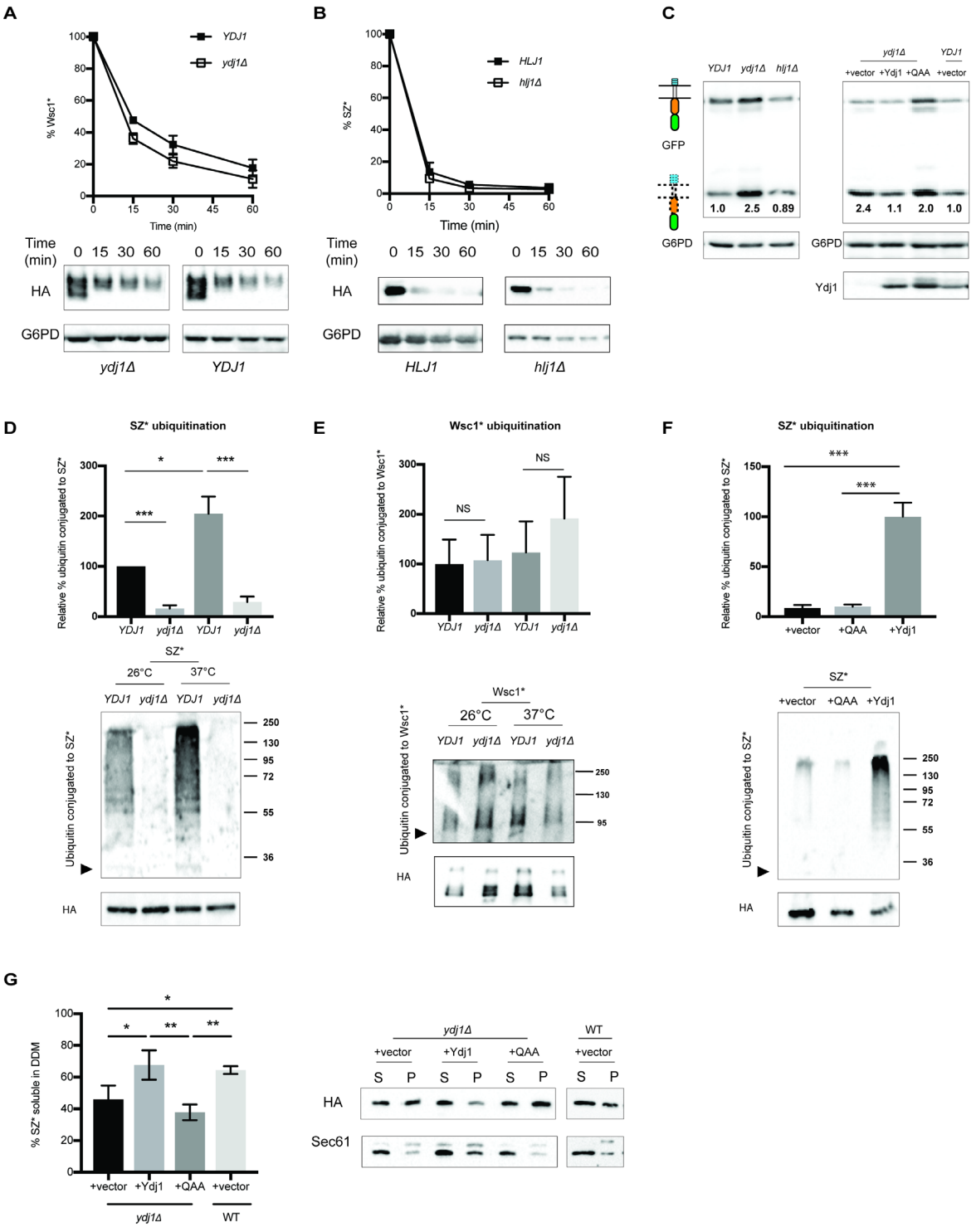

Figure S2. The cytosolic Hsp40, Ydj1, facilitates the ER retention of SZ* through substrate ubiquitination. Related to Figure 1 and 2. (A) The stability of Wsc1* in wild-type and *ydj1Δ* yeast was determined by cycloheximide chase assay. Data represent the means ± SE of 3 independent experiments. (B) The stability of SZ* in

wild-type and *hlj1Δ* yeast was determined by cycloheximide chase. Data represent the means ± SE of 3 independent experiments. (C) Left: GFP cleaved from SZ*-GFP was determined by immunoblotting in a wild-type yeast strain or in a strain lacking Hlj1 or Ydj1. Right: Numbers indicate average values of normalized cleaved GFP from 2-3 independent experiments. GFP cleaved from SZ*-GFP was determined by immunoblotting in a *YDJ1* strain with a vector control or the *ydj1Δ* yeast strain containing a vector control or expressing Ydj1 or Ydj1-QAA as well as SZ*-GFP. As a control SZ*-GFP was expressed in wild-type yeast containing the vector control. In this experiment, the level of exogenous Ydj1 or the QAA mutant in the delete background was ~50% higher than in the wild-type strain. Ubiquitination of SZ* (D) and Wsc1* (E) in wild-type and *ydj1Δ* yeast was examined by immunoprecipitation under denaturing conditions. Cultures were shifted to 37°C or remained at 26°C for 30 min prior to harvesting. SZ* (HA, in part D) and Wsc1* (HA, in part E) as well as ubiquitinated substrate are shown. The closed arrowhead on the left represents the location at which SZ* and Wsc1* migrate, and a molecular mass ladder ($x10^{-3}$ Dalton) is shown to the right. (F) Ubiquitination of SZ* from *ydj1Δ* yeast expressing SZ* and the indicated insert in a *CEN* plasmid were detected by denaturing immunoprecipitation of SZ*. The QAA mutant lacks the Hsp70-interacting HPD motif. SZ* (HA) was detected as well as ubiquitinated substrate. (G) Microsomes from *ydj1Δ* yeast expressing SZ* and vector/Ydj1 /Ydj1-QAA were treated with 1% dodecyl maltoside (DDM). As a control, microsomes from wild-type yeast expressing SZ* and containing the vector control was also tested. Protein residing in the supernatant (S) and pellet (P) fractions was analyzed after centrifugation and immunoblotting. Sec61 (bottom band in the doublet) was blotted as a control. Data represent the means ± SE of 3 independent experiments; * $p<0.05$, ** $p<0.005$, *** $p<0.0005$, NS: non-significant.

Figure S3

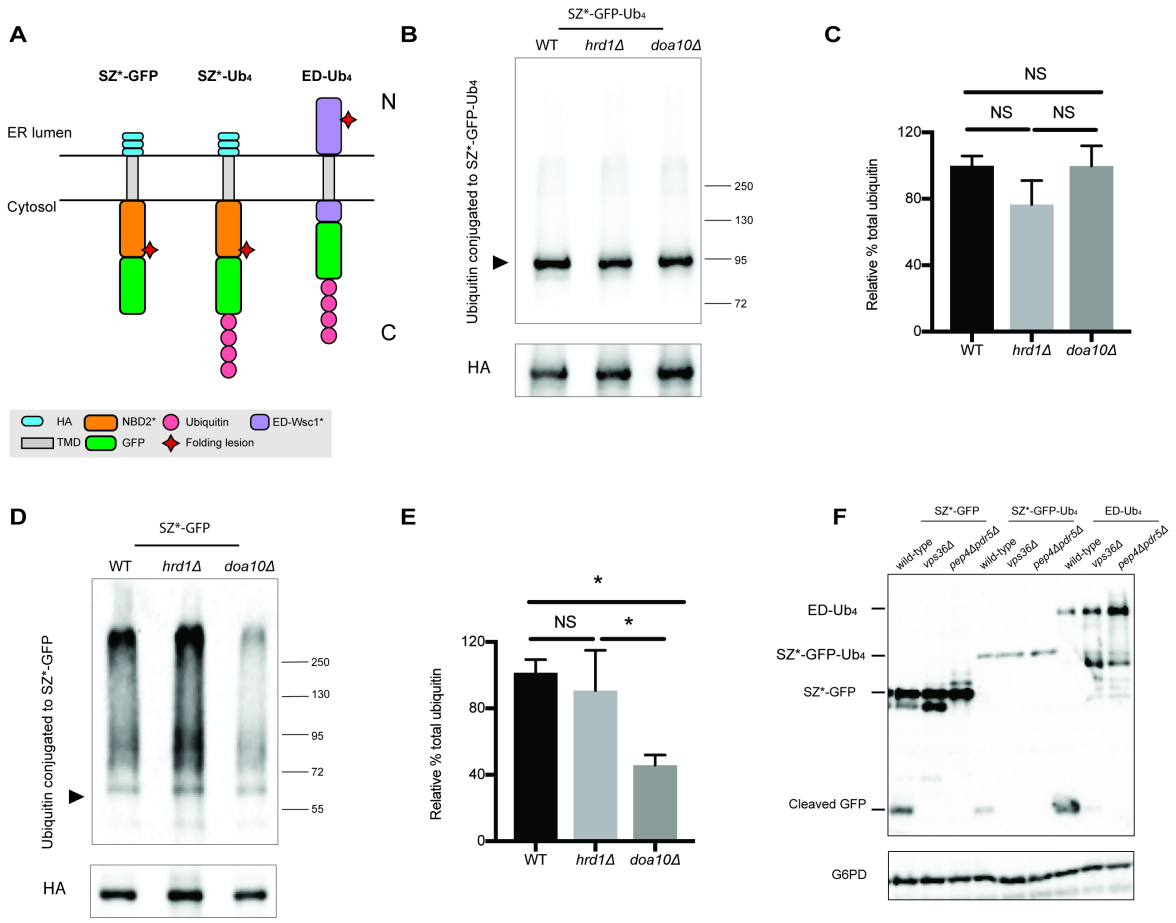

Figure S3. Comparison of SZ*-GFP and SZ*-GFP ubiquitination. Related to Figure 3, 4 and 7 (A) Schematic of SZ*-GFP, SZ*-GFP-Ub_4, and ED-Ub_4. N and C indicate the topology with respect to the ER. Ubiquitination of SZ*-GFP-Ub_4 (B) and SZ*-GFP (D) in wild-type, *hrd1Δ,* and *doa10Δ* yeast was examined by immunoprecipitation under denaturing conditions. The signals corresponding to SZ*-GFP (HA) (C) and SZ*-GFP-Ub_4 (HA) (E) are also shown. The arrowhead to the left represents the location at which the indicated substrates migrate, and a molecular mass ladder ($x10^{-3}$ Dalton) is shown to the right. Bar graphs (C) and (E) depict the ubiquitin signals quantified from (B) and (D), respectively. Data represent the means ± SE of 3 independent experiments; NS: nonsignificant. (F) GFP cleavage in the wild-type and indicated mutant strains was determined by immunoblotting.

Figure S4

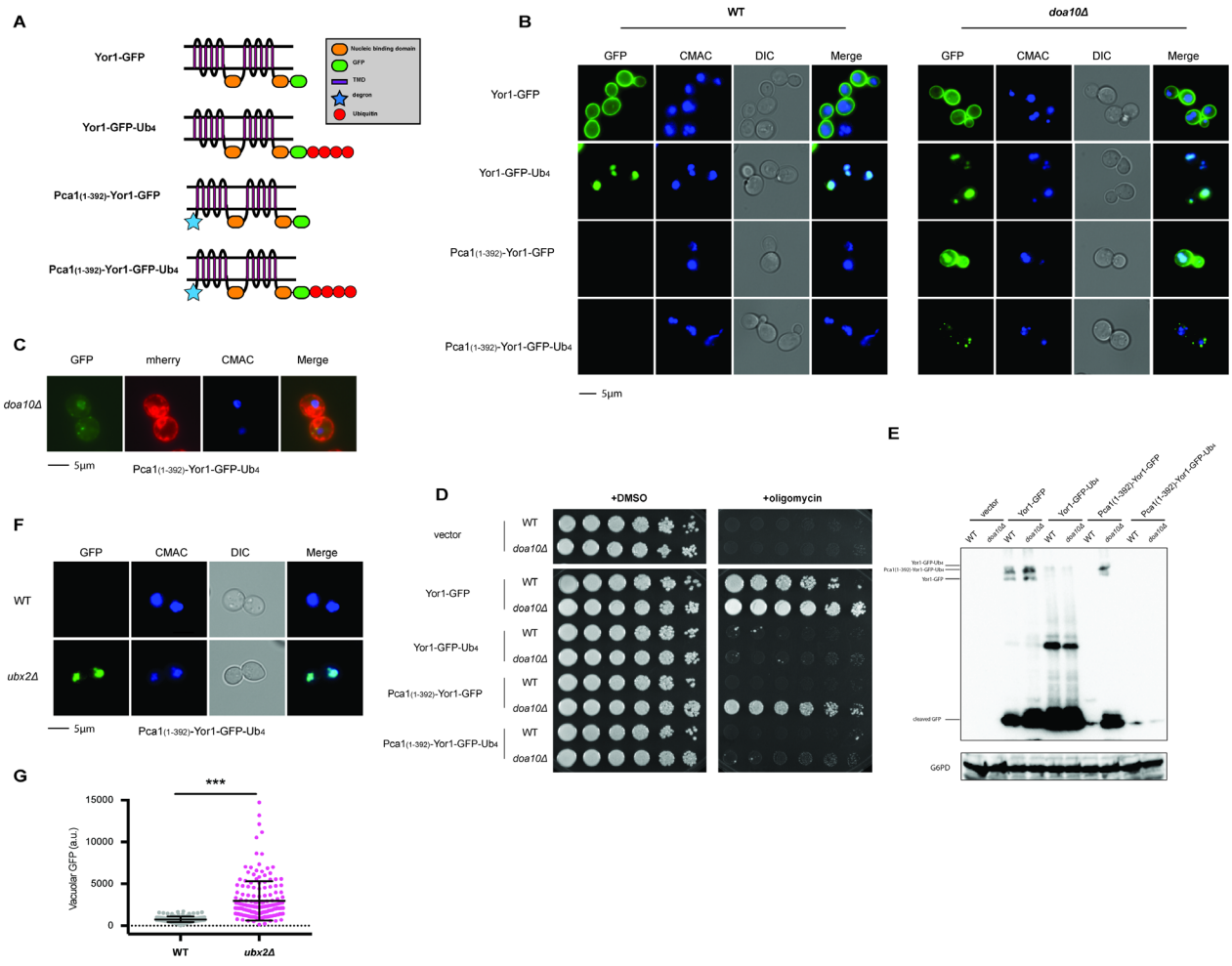

Figure S4. A linear tetra-ubiquitin motif is sufficient to retain a misfolded but not a native membrane protein in the ER. Related to Figure 4 and 7. (A) Schematic of Yor1-GFP, Yor1-GFP-Ub$_4$, Pca1(1-392)-Yor1-GFP, and Pca1(1-392)-Yor1-GFP-Ub$_4$. (B) Live-cell fluorescence imaging of Yor1-GFP, Yor1-GFP-Ub$_4$, Pca1(1-392)-Yor1-GFP, and Pca1(1-392)-Yor1-GFP-Ub$_4$ in wild-type and *doa10Δ* yeast. CMAC marks the yeast vacuole. (C) Live cell fluorescence imaging of *doa10Δ* yeast expressing the integrated fluorescent marker mCherry-Scs2-tm (ER-cherry) and Pca1(1-392)-Yor1-GFP-Ub$_4$. Note the presence of ER resident puncta. (D) Oligomycin resistance of wild-type or *doa10Δ* yeast containing a vector control or expressing Yor1-GFP, Yor1-GFP-Ub$_4$, Pca1(1-392)-Yor1-GFP, or Pca1(1-392)-Yor1-GFP-Ub$_4$. Cells were spotted on YPEG agar media containing 2.5μg/ml oligomycin or DMSO as control. Cell growth was monitored 5 days after spotting. (E) Steady-state level of Yor1-GFP, Yor1-GFP-Ub$_4$, Pca1(1-392)-Yor1-GFP, and Pca1(1-392)-Yor1-GFP-Ub$_4$ in wild-type and *doa10Δ* yeast was determined by immunoblotting. (F) Live-cell fluorescence imaging of Pca1(1-392)-Yor1-GFP-Ub$_4$ in wild-type and *ubx2Δ* yeast. (G) Quantification of GFP intensity in the vacuole in (F). Greater than 100 cells in each strain were counted; *** $p<0.0005$. a.u.: arbitrary units.

Figure S5

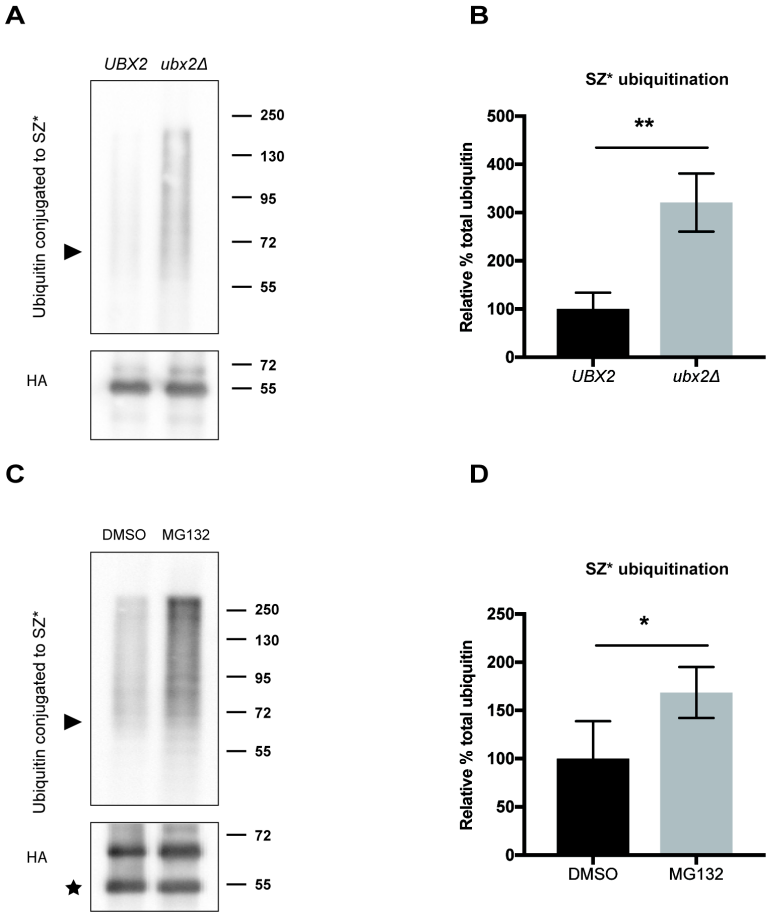

Figure S5. SZ* is efficiently ubiquitinated in yeast lacking Ubx2 or when the proteasome is inhibited. Related to Figure 5. (A) SZ*-GFP ubiquitination was examined in the presence or absence of Ubx2 by immunoprecipitation of SZ*-GFP under denaturing conditions. SZ*-GFP (HA) is shown as well as total ubiquitin. The arrowhead to the left represents the location at which SZ* migrates, and a molecular mass ladder (x10^{-3} Dalton) is shown to the right. (B) A bar graph depicts the ubiquitin signal quantified from (A). Data represent means ± SE of 3 independent experiments; ** $p<0.005$. (C) SZ*-GFP ubiquitination was examined in the presence or absence of the proteasome inhibitor, MG132, in *pdr5Δ* yeast. Cells were grown in the presence or absence of MG132 for 30 min prior to harvest. The star denotes a faster migration population of SZ*-GFP due to partially denatured GFP. (D) A bar graph depicts the ubiquitin signal quantified from (C). Data represent the means ± SE of 3 independent experiments; * $p<0.05$.

Figure S6

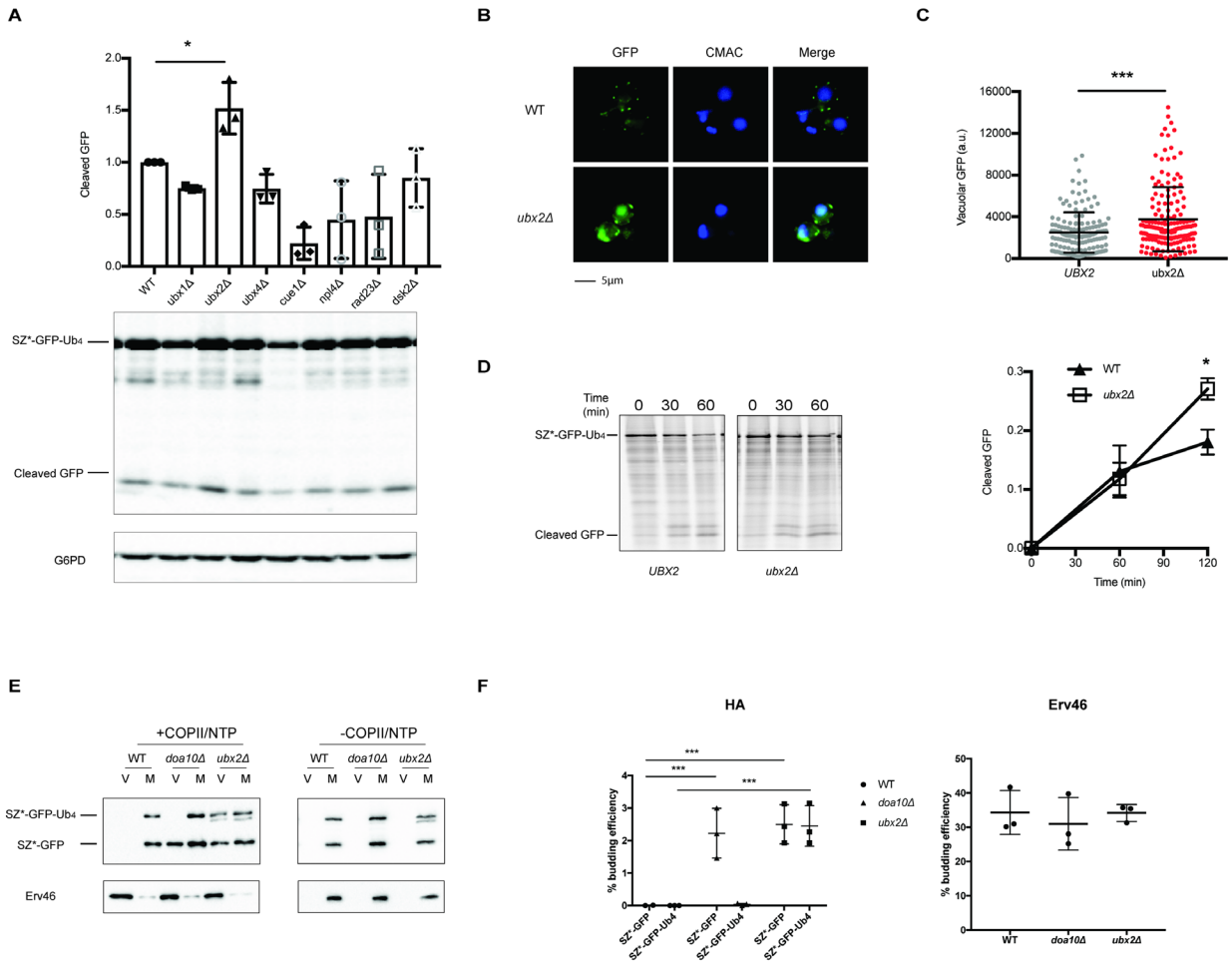

Figure S6. Loss of the Ubx2 facilitates the ER exit of SZ*-GFP-Ub$_4$. Related to Figure 3, 4 and 5. (A) GFP cleavage from SZ*-GFP-Ub$_4$ in the wild-type and the indicated UBA mutant strains was determined by immunoblotting. Data represent the means ± SE of 3 independent experiments; *p<0.05. (B) Live-cell fluorescence imaging of SZ*-GFP-Ub$_4$ in wild-type and *ubx2Δ* yeast. CMAC marks the yeast vacuole. (C) Quantification of GFP intensity in the vacuole of SZ*-GFP in (B). Greater than 100 cells in each strain were counted; *** p<0.0005. (D) The GFP cleavage rate was measured by pulse-chase in wild-type and *ubx2*Δ yeast. Cleavage was determined by normalizing free GFP to full-length SZ*-GFP-Ub$_4$ at 0 min. Data represent the means ± SE of 3 independent experiments; * p<0.05. (E) The simultaneous *in vitro* COPII budding efficiency of SZ*-GFP and SZ*-GFP-Ub4 in the presence or absence of Doa10 or Ubx2, respectively, was measured. Microsomes were prepared from the indicated yeast strains co-expressing SZ*-GFP and SZ*-GFP-Ub4. V: 50% of total budded vesicles, M: 2.5% unbudded microsomes used in the reaction. +COPII/NTP and -COPII/NTP indicate experiments performed in the presence or absence of the purified COPII proteins and energy, respectively. (F) A graph depicts *in vitro* budding efficiency of SZ*-GFP as quantified from (E). Data represent the means ± SE of 3 independent experiments; ***p<0.0005.

Figure S7

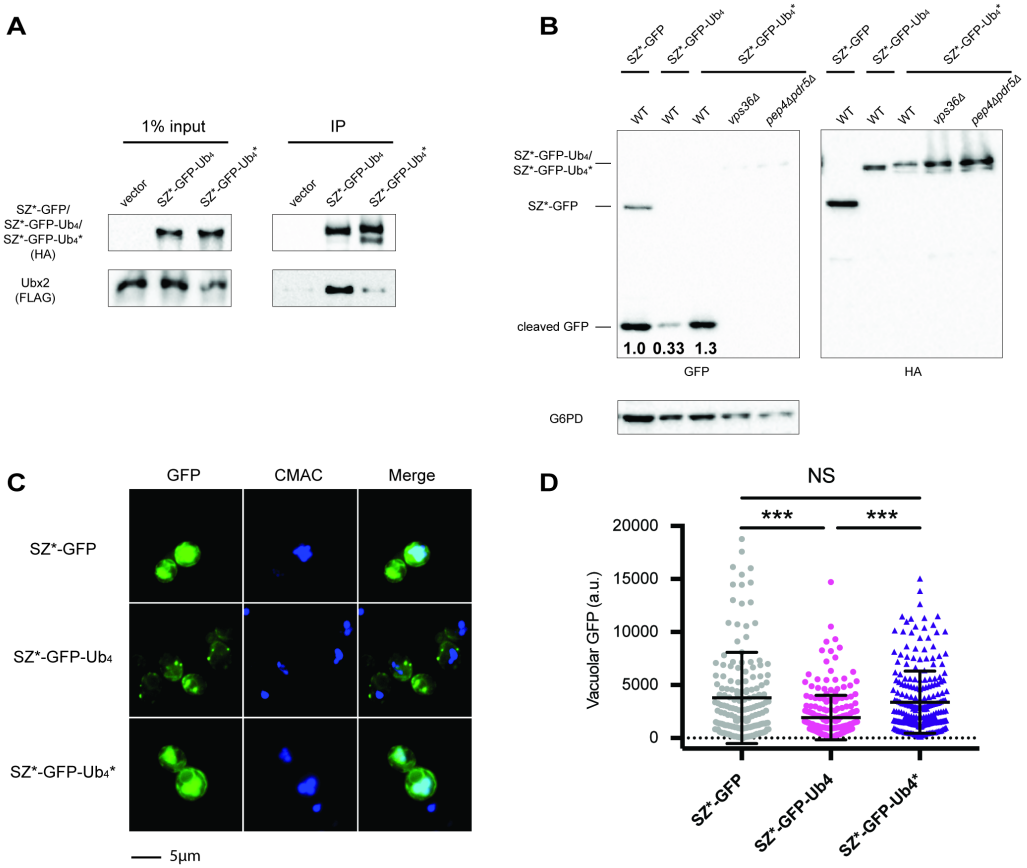

Figure S7. ER retention conferred by linear tetraubiquitin is governed by the interaction between Ubx2 and ubiquitin. Related to Figure 5 and 6. (A) Vector control and HA-tagged SZ*-GFP-Ub_4/SZ*-GFP-Ub_4* were immunoprecipitated from wild-type yeast expressing the indicated substrates. After SDS-PAGE, the indicated antibodies were used to detect SZ*-GFP-Ub_4, SZ*-GFP-Ub_4* and Ubx2, which was FLAG-tagged. 1% of the input was analyzed to show equal loading. (B) GFP cleaved from SZ*-GFP, SZ*-GFP-Ub_4, or SZ*-GFP-Ub_4* was determined by immunoblotting in wild-type and the indicated mutant yeast strains. Numbers indicate average values of normalized cleaved GFP from 3 independent experiments. The top left panel shows a western blot for GFP, and right panel shows western blot for HA (to detect the SZ* backbone). The incomplete visualization of the Ub_4 species with the anti-GFP antibody was due to an obscured epitope when the tetra-ubiquitin was present. (C) Live-cell fluorescence imaging of SZ*-GFP, SZ*-GFP-Ub_4, or SZ*-GFP-Ub_4* in wild-type yeast. CMAC marks the yeast vacuole. (D) Quantification of GFP intensity in the vacuole of SZ*-GFP, SZ*-GFP-Ub_4, or SZ*-GFP-Ub_4* in (C). More than 100 cells in each strain were counted; *** $p<0.0005$, NS: nonsignificant. a.u.: arbitrary units.

Figure S8

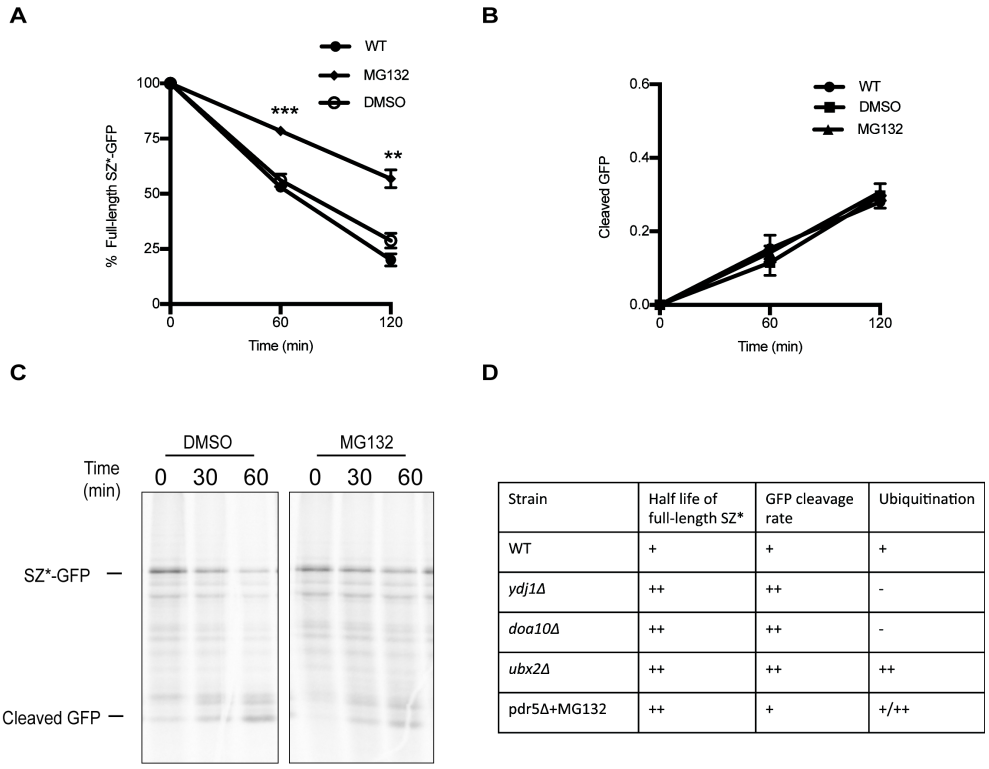

Strain	Half life of full-length SZ*	GFP cleavage rate	Ubiquitination
WT	+	+	+
ydj1Δ	++	++	-
doa10Δ	++	++	-
ubx2Δ	++	++	++
pdr5Δ+MG132	++	+	+/++

Figure S8. Proteasome inhibition in unable to improve the ER exit of SZ*. Related to Figure 2, 3 and 5. The stability of SZ*-GFP (A) and GFP cleavage (B) were measured by pulse-chase in *pdr5Δ* yeast treated in the presence or absence of the proteasome inhibitor MG132. Cleavage was determined by normalizing free GFP to full-length SZ*-GFP at 0 min. Data represent the means ± SE of 3 independent experiments. ** $p<0.005$, *** $p<0.0005$. (C) Representative data used for (A) and (B). (D) Summary of the SZ*-GFP half-life and GFP cleavage derived from pulse chase data and SZ* ubiquitination.